Eur Biophys J (1994) 22:405–421

European Biophysics Journal


# A model of microtubule oscillations

**A. Marx, E. Mandelkow**

Max-Planck-Unit for Structural Molecular Biology, c/o DESY, Notkestrasse 85, D-22603 Hamburg, Germany

Received: 13 April 1993 / Accepted in revised form: 5 October 1993

**Abstract.** Simulations of microtubule oscillations have been obtained by a kinetic model including nucleation of microtubules, elongation by addition of GTP-loaded tubulin dimers, disassembly into oligomers, and dissolution of oligomers followed by nucleotide exchange at the free dimers. Dynamic instability is described by the on and off rates for dimer association in the growth phase, the rate of rapid shortening, and the transition rates for catastrophe and rescue. The latter are assumed to be completely determined by the current state of the system ("short cap hypothesis"). Microtubule oscillations and normal polymerizations measured by time-resolved X-ray scattering were used to test the model. The model is able to produce oscillations without further assumptions. However, in order to obtain good fits to the experimental data one requires an additional mechanism which prevents rapid desynchronization of the microtubules. One of several possible mechanisms that will be discussed is the destabilization of microtubules by the products of disassembly.

**Key words:** Dynamic instability – Cap model – Cooperativity – Synchronization – Small angle X-ray scattering – Cytoskeleton

## I. Introduction

Microtubules (MTs) in the state of growth (G-MTs) and MTs in the state of shortening (S-MTs) can coexist in solution, and they can change their dynamic state by stochastic transitions. This phenomenon has been called "dynamic instability" (Mitchison and Kirschner 1984). It has been observed directly by video-enhanced light-microscopy of single MTs in vitro (Horio and Hotani 1986; Walker et al. 1988) as well as in vivo (Cassimeris et al. 1988; Sammak and Borisy 1988; Schulze and Kirschner 1988). Dynamic instability is important for the functions of MTs in the living cell. It allows adaptation of the cytoskeleton to changing requirements, and it is an essential ingredient of the mitotic apparatus. A number of experimental studies were directed to the quantification of dynamic instability in vitro (Walker et al. 1988, 1991; O'Brien et al. 1990; Drechsel et al. 1992; Gildersleeve et al. 1992; Pryer et al. 1992; Trinczek et al. 1993). In its simplest form, dynamic instability is described by the rates of growth and shortening, and the rates of transitions from the growth state to the shortening state ("catastrophe") and vice versa ("rescue").

Virtually all models of dynamic instability start from the assumption that the interior of MTs, which consists mainly of TU · GDP, is unstable and that immediate decay of growing MTs is prevented by the presence of stabilizing caps (Erickson and O'Brien 1992). The nature of the caps is still a matter of debate. Early models assumed extended caps of TU · GTP (Carlier and Pantaloni 1981; Hill and Chen 1984; Chen and Hill 1985): since MTs elongate by association of TU · GTP, spontaneous hydrolysis of the incorporated GTP at a rate smaller than the rate of elongation would automatically result in an extended "GTP-cap", with the concentration of TU · GTP gradually decreasing from the tip to the core ("uncoupled stochastic hydrolysis" model; see Stewart et al. 1990). In the "uncoupled vectorial hydrolysis" model, the cap consists of pure TU · GTP and hydrolysis takes place only at the interface between cap and core. Later, Carlier et al. (1988) proposed that the transition from stable to unstable conformations might be coupled to the release of phosphate ($P_i$), not to the hydrolysis of GTP. Thus, growing MTs would be stabilized by a GDP · $P_i$-cap instead of a GTP-cap. However, extended caps of any form seem to be excluded by a number of experiments (O'Brien et al. 1987; Schilstra et al. 1987;

*Abbreviations:* MT(s), microtubule(s); G-MT/S-MT, microtubule in the state of growth/shortening; GTP, guanosine 5′-triphosphate; GDP, guanosine 5′-diphosphate; TU · GDP/TU · GTP, tubulin dimer with GDP/GTP bound to the exchangeable nucleotide binding site; MAP(s), microtubule-associated protein(s); PC, tubulin phosphocellulose-purified tubulin; PIPES, piperazine-1,4-bis(2-ethane sulfonic acid); DDT, dithiothreitol; EGTA, ethylene glycol-O,O′-bis(2-amino ethyl ether)-N,N,N′,N′-tetraacetic acid

*Correspondence to:* A. Marx

Stewart et al. 1990; Walker et al. 1991; Voter et al. 1991; Caplow 1992).

In the Lateral Cap model (Bayley et al. 1989a, 1990; Martin et al. 1991, 1993), the cap is restricted to a single layer of TU · GTP at the ends of the MTs. Hydrolysis of GTP is coupled to the association of TU · GTP. There is an essential difference between extended cap models and models with short caps, independent of the nature of the cap: in "short cap" models[1], the catastrophe rate depends only on current buffer conditions, whereas in extended cap models it depends also on the growth history. Though the Lateral Cap model provides an attractive kinetic mechanism, additional factors cannot be excluded. For instance, the stability of MTs may be controlled by the conformational state of the terminal dimers in addition to the state of nucleotide hydrolysis (conformational cap hypothesis; Stewart et al. 1990; Caplow 1992).

MT dynamics can also be studied by using solution scattering techniques to probe the behavior of a large population of MTs simultaneously. Light scattering (turbidity measurements; Gaskin et al. 1974) and X-ray scattering have been used (Mandelkow et al. 1980, 1983). The advantage of X-ray scattering over turbidity measurements is that the MT signal can be separated from that of concurrent structures. Tubulin in standard reassembly buffer (0.1 mM PIPES, pH 6.9 with typically 1 or 2 mM GTP and equimolar $Mg^{++}$) polymerizes in an apparently monotonic fashion. At high protein concentrations, oscillations of the extent of polymerization have been observed in various buffer conditions (Carlier et al. 1987; Pirollet et al. 1987; for review see: Mandelkow and Mandelkow 1992). One can distinguish between two types of oscillations, depending on the presence or absence of exogenous GTP. In the latter case, GTP is regenerated enzymatically from endogenous GDP (Pirollet et al. 1987; Wade et al. 1989). The periodicities of these oscillations depend on the efficiency of the GTP regeneration system. In most experiments, however, exogenous GTP is supplied by adding one or several mM to the initial solution. Under these conditions, tubulin assembly can follow its own rhythm, though oscillations will be damped due to the consumption of GTP. In the present work, only tubulin assembly at high concentrations of GTP will be considered.

It is evident that dynamic instability provides the fundamental basis for oscillations. By numerical simulations, it could be shown, that dynamic instability of individual MTs, together with slow regeneration of TU · GTP from disassembling MTs, can indeed provoke oscillations (Carlier et al. 1987; Chen and Hill 1987; Lange et al. 1988; Bayley et al. 1989). Striking differences between calculated and measured oscillations were not surprising because of the simplifications and approximations used in the simulations. Thus, the calculations did not answer the question whether or not dynamic instability is sufficient to understand real oscillations.

[1] In the following, the term "short cap" is used with the connotation of MTs without memory, although conceptually, the pair of opposites "extended cap MT/short cap MT" should be distinguished from "MT with/without memory"

In this work, we present a more quantitative mathematical model for MT polymerization kinetics in bulk solutions. It is based on the reaction cycle described by Mandelkow et al. (1988) and on the assumption that the catastrophe rate depends only on the current state of the system (not on the growth history). This means that transitions from growth to shortening are controlled by a "short cap" (without specifying the details of the mechanism). We used this model to simulate real oscillations and normal polymerizations observed by time-resolved solution scattering of synchrotron radition. It turned out that satisfactory simulations can be achieved only by the postulation of an additional mechanism that serves to retard desynchronization of the MTs.

## II. Materials and methods

### *a) Tubulin preparation*

MT-protein with about 20 weight-% MAPs and phosphocellulose-purified tubulin (PC-tubulin) without MAPs were prepared from pig brain as described (Mandelkow et al. 1985). Protein concentrations were determined by the BCA method (Smith et al. 1985) using bovine serum albumin as standard.

### *b) Small angle X-ray scattering*

Polymerization of MTs in tubulin solutions was initiated by a rapid temperature jump from 4 °C to 37 °C and observed by time-resolved small angle X-ray scattering. The experiments were performed on instrument X33 of the EMBL Outstation at the DESY synchrotron laboratory, Hamburg (Koch and Bordas 1983; Boulin et al. 1986). Tubulin solutions were placed in a 1 mm pathlength cell covered with 50 μm thick mica windows. The cell was equipped with a T-jump apparatus (Renner et al. 1983), allowing rapid changes from 4 °C to 37 °C with half-times of 8 seconds. Accumulation time per frame was 3 seconds. Scattering angles were calibrated against collagen from rat tendon (64 nm repeat assumed).

### *c) Data analysis*

The analysis of the scattering patterns follows the treatment described previously (Mandelkow et al. 1980, 1988; Lange et al. 1988). Scattering patterns of solutions containing large quantities of MTs have characteristic maxima at $\approx 0.05\ nm^{-1}$ and $\approx 0.09\ nm^{-1}$ (curves "MT" in Fig. 1). Before polymerization, scattering patterns are either flat (curves "DI" in Fig. 1a, b, typical for tubulin dimers) or have weak maxima at $\approx 0.035$ and $0.06\ nm^{-1}$ (curves "OL" in Fig. 1c, d, indicating the presence of oligomers).

A remarkable feature of the curves in Fig. 1 is the presence of points of nearly constant intensity ("quasi-isosbestic" points). This holds for both, PC-tubulin (Fig. 1a, b) and MT-protein (Fig. 1c, d). Isosbestic points are typical of two-component systems. However, in the processes of MT polymerization and oscillation several

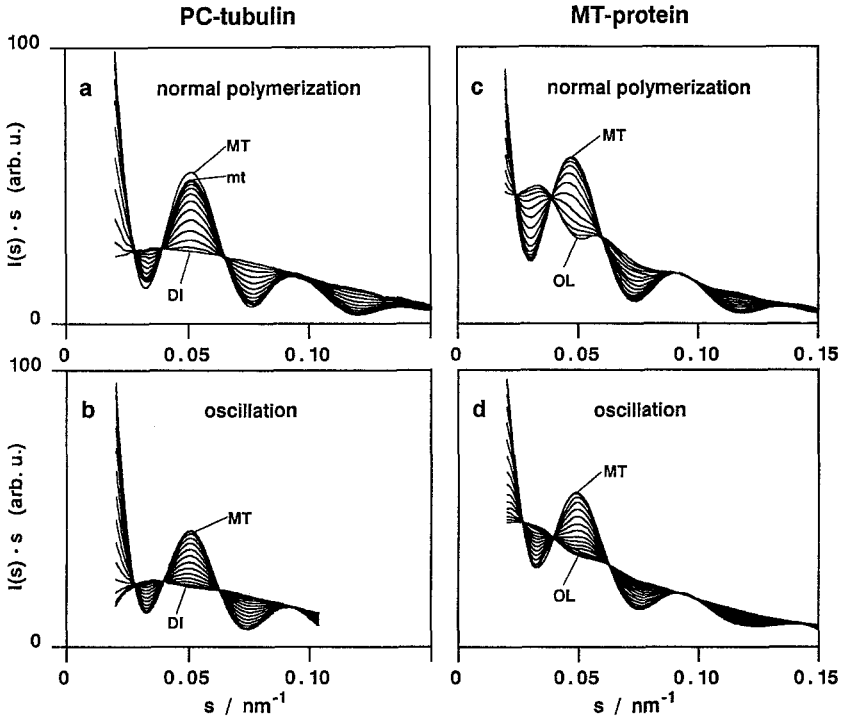


**Fig. 1a–d.** X-ray scattering patterns ($I(s) \cdot s$ versus $s$) of tubulin solutions recorded during polymerization. I: scattering intensity, $s$: Bragg spacing ($s = 2\sin(\vartheta)/\lambda$, $2 \cdot \vartheta$ = scattering angle). Accumulation time per scattering pattern was 3 s. The solvent scattering has been subtracted and the results have been smoothed by use of a cubic spline. Only patterns between the beginning of MT polymerization and attainment of the maximal extent of polymerization (first maximum for oscillations) are shown. **a** and **b** normal (monotonic) polymerization and oscillation in solutions of MAP-free tubulin (PC-tubulin); **c** and **d** analogous for MT-protein containing MAPs. The scattering patterns of solutions with high contents of MTs ("MT") have characteristic maxima at about 0.05 $nm^{-1}$ and 0.09 $nm^{-1}$. The scattering patterns recorded immediately before MT polymerization are either smooth ("DI", in the case of PC tubulin, **a** and **b**) or show weak maxima or shoulders at about 0.035 $nm^{-1}$ and 0.06 $nm^{-1}$ ("OL", in the case of MT-protein, **c** and **d**). Smooth patterns with low near-center scattering are typical for solutions containing tubulin dimers. The maxima at 0.035 and 0.06 $nm^{-1}$ indicate that a certain amount of oligomer rings with diameters of about 35 nm is still present at the onset of polymerization. (These maxima are more pronounced in the scattering patterns recorded before and immediately after the temperature jump; not shown) A mixture of incomplete rings and small aggregates of dimers may also be present, though these oligomers will only give rise to additional "background" scattering. **a** 36 mg/ml PC tubulin in 100 mM PIPES at pH 6.9, 2 mM GTP, 2 mM $MgCl_2$, 1 mM DTT. Between the scattering patterns "mt" and "MT" shown in **a**, 16 patterns (48 s) have been skipped. **b** 31 mg/ml PC-tubulin in 100 mM PIPES at pH 6.9, 7 mM GTP, 20 mM $MgCl_2$, 60 mM NaCl, 1 mM DTT. The range between $s \approx 0.10$ $nm^{-1}$ and 0.15 $nm^{-1}$ was not measured. **c** 30 mg/ml MT-tubulin ($C_4S$) in 100 mM PIPES at pH 6.9, 2mM GTP, 2 mM $MgCl_2$, 7 mM DTT. **d** 31 mg/ml MT-protein ($C_4S$) in 100 mM PIPES at pH 6.9, 5 mM GTP, 20 mM $MgCl_2$, 60 mM NaCl, 5 mM DTT. The change of intensity at 0.05 $nm^{-1}$ (first maximum of MT scattering) was used to calculate the extent of MT polymerization. For variations of the extent of polymerization with time see Figs. 2 and 3

components are involved (dimers, oligomers of various sizes including ring oligomers, and MTs). The existence of quasi-isosbestic points in such mixtures may be explained by the combination of several effects: (*i*) The scattering patterns of species B, C, D, ... all have a similar form, which is quite different from the pattern of species A. (*ii*) The relative concentrations of species B, C, D, ... do not change much during the course of the reaction. (*iii*) The two-component-like behavior is not altered by the presence of other components whose concentrations remain constant, either because they are not involved in the reaction (e.g. free MAPs) or because production and decomposition are compensating each other.

As a consequence of the two-component-like behavior, the contribution of MTs can easily be separated: The relative extent of MT-polymerization at a given time is to a good approximation proportional to the difference between the scattering at that time and the scattering before the beginning of polymerization (best measured at the Bragg spacing of the first MT maximum). Deviations from the regular behavior of two-component systems are visible in the near-center region at Bragg spacings around and below 0.035 $nm^{-1}$ (close to the first maximum of the oligomer pattern). There, the difference between oligomer and dimer scattering is most prominent. However, quantitative separation of components other than MTs is very unreliable. For this reason, we consider only the time course of the extent of MT-polymerization.

Absolute values for the extent of polymerization (the concentration of tubulin dimers incorporated in MTs) were obtained as follows: The maximum extent of the normal polymerizations shown in Fig. 1a (PC-tubulin) and Fig. 1b (MT-protein) was assumed to be 95% (assuming a critical dimer concentration of about 2 mg/ml) and 100% (complete polymerization), respectively. The scattering patterns shown in Fig. 1a, c were used as reference standards for other measurements. For instance, the absolute extent of polymerization for the oscillation shown in Fig. 1b was determined by comparing the scattering at the maximum of the first cycle ("MT" curve in

Fig. 1b) with the curves in Fig. 1a. Variations in the intensity scales between different experiments were accounted for by matching the scattering patterns recorded before the beginning of polymerization. Because of variations between the scattering patterns of different samples, the accuracy of the absolute values obtained by this method is limited to about $\pm 10\%$.

## III. Theory

The time course of all relevant concentrations is described by a set of ordinary differential equations, based on the law of mass action, with time not being included as an explicit variable (Table 1). According to the reaction cycle described earlier (Mandelkow et al. 1988), these equations include terms for spontaneous nucleation and dissolution of MTs, elongation in the growing phase, spontaneous transitions from growth to shortening (catastrophe) and from shortening to growth (rescue), depolymerization of S-MTs into oligomers, disintegration of oligomers into TU · GDP, and exchange of nucleotides at the dimer level to form TU · GTP.

The system of equations in Table 1 (hereafter referred to by "MTOSC") is a minimal model in the sense that it includes only those reactions considered to be essential for a consistent simulation of MT oscillations. Many complicating features have been neglected for the sake of practicability. The model could easily be modified by introducing additional terms, but at the expense of obscuring the principal mechanisms (see Discussion).

### *MT polarity*

MTs are formally treated as linear polymers with only one active end. For describing the differences between plus and minus ends, most of the kinetic parameters would have to be doubled. Thus, treadmilling, for instance, is beyond the scope of the model. This seems not to be a serious drawback as the parameters used in the calculations can be understood as combinations of the actual plus and minus end parameters. For example, the rates $k_+$ and $k_-$ of dimer association and dissociation in the growing state should be considered as the sums of the corresponding rates for plus and minus ends; the rate of depolymerization, $k_{depol}$, should be an appropriate mean value because depolymerization will normally occur only from one end. With regard to the question about the source of synchrony in MT oscillations one can say that if synchronization is difficult to achieve with only one type of MT-ends, it will be even more difficult with two.

### *Nucleation and catastrophe*

In real oscillations, the MT number concentration varies by nucleation and total decay of S-MTs. Nucleation and catastrophe are the nonlinear steps required for oscillations. By theoretical concepts and experimental observation, they are assumed to be strongly dependent on the concentration of TU · GTP. We use exponential functions, $k_{nuc}$ and $k_{cat}$, to describe the TU · GDP dependence of nucleation and catastrophe. We tested other types of dependences but found little effect on the predictions of the model, as long as the functions are assumed to be continuous and monotonic in the TU · GTP concentration.

The main result of our calculations is that oscillations like those shown in Fig. 2 cannot be simulated without

**Table 1.** MTOSC system of differential equations

$$
\begin{aligned}
(1)\ \dot{c}_G &= k_{nuc} - k_{cat} c_G + k_{resc} c_S \\
(2)\ \dot{c}_S &= k_{cat} c_G - k_{resc} c_S - k_{depol} \frac{c_S^2}{c_{shr}} \\
(3)\ \dot{c}_{shr} &= k_{cat} c_{grw} - k_{resc} c_{shr} - k_{depol} c_S \\
(4)\ \dot{c}_{oli} &= k_{depol} c_S - k_{oli} c_{oli} \\
(5)\ \dot{c}_{ina} &= k_{oli} c_{oli} - k_{exc} c_{exc} \\
(6)\ \dot{c}_{act} &= k_{exc} c_{exc} - (k_+ c_{act} - k_-) c_G \\
(7)\ \dot{c}_{GTP} &= -k_{spon} c_{GTP} - k_{exc} c_{exc}
\end{aligned}
$$

with:

$$
k_{nuc} := q_{nuc} \exp\left(\frac{c_{eff} - z_{nuc}}{s_{nuc}}\right) \qquad c_{eff} := c_{act} \exp(-g(c_{oli} + c_{ina}))
$$

$$
k_{cat} := q_{cat} \exp\left(\frac{z_{cat} - c_{eff}}{s_{cat}}\right) \qquad c_{exc} := c_{ina} - \frac{c_{act} + c_{ina}}{r \dfrac{c_{GTP}}{c_{GXP} - c_{GTP}} + 1}
$$

$$
c_{grw} := c_{tot} - c_{oli} - c_{ina} - c_{act} - c_{shr}
$$

Equations (1) to (7) define the time derivatives of the seven independent variables listed here: $c_G, c_S$: molar number concentrations of MTs in the $G$ (growing) and $S$ (shortening) state, respectively (one end per microtubule assumed, see text). $c_{shr}, c_{oli}, c_{ina}, c_{act}$: molar concentrations of dimers in the form of $S$-MTs ($c_{shr}$), of oligomers ($c_{oli}$), of TU · GDP ("inactive" dimers, $c_{ina}$), and of TU · GTP ("active" dimers, $c_{act}$). $c_{GTP}$: molar concentration of free $Mg^{++}$-GTP. The following variables, used in the differential equations and throughout this work, are combinations of the above defined variables: $c_{grw}$: molar concentration of dimers in the form of $G$-MTs (assumption: $c_{grw} + c_{shr} + c_{oli} + c_{ina} + c_{act} = c_{tot} = \text{const}$). $c_{eff}$: effective concentration of TU · GTP for nucleation and catastrophic transitions (see text). $c_{exc}$: difference between $c_{GTP}$ and the instantaneous steady state concentration of free $Mg^{++}$-GTP. $c_{MT} := c_G + c_S$, total microtubule number concentration. $c_{pol} := c_{grw} + c_{shr}$, total concentration of dimers in the form of microtubules ("extent of polymerization"). $c_{GDP} := c_{GXP} - c_{GTP}$: molar concentration of free $Mg^{++}$-GDP. MTOSC contains 12 independent kinetic and 3 general parameters: $q_{nuc}, z_{nuc}, s_{nuc}$: parameters defining the concentration dependence of the zero order nucleation rate constant $k_{nuc}$. Only two of the parameters are independent of each other; the given form of the function $k_{nuc}$ was chosen for convenience. $q_{cat}, z_{cat}, s_{cat}$: parameters defining the concentration dependence of the first order catastrophe rate constant, $k_{cat}$. Only two of the parameters are independent of each other. $k_{resc}$: first order rescue rate constant. $k_{depol}$: first order rate constant of $S$-MT depolymerization (in dimer equivalents). $k_+, k_-$: second order dimer association and first order dimer dissociation rate constant of $G$-MTs, respectively (assumption: association and dissociation of TU · GTP only). $k_{oli}$: first order rate constant of oligomer into dimer conversion. $k_{exc}$: nucleotide exchange rate constant. $r$: relative affinity of the $Mg^{++}$-nucleotide complexes to the exchangeable nucleotide binding site of the tubulin dimer ($r = K_{GTP}/K_{GDP}$, with $K_{GTP}, K_{GDP}$ equilibrium association constants of $Mg^{++}$-GTP and $Mg^{++}$-GDP, respectively). $k_{spon}$: first order rate constant of spontaneous hydrolysis of free $Mg^{++}$-GTP. $c_{tot}$: total molar concentration of tubulin dimers. $c_{GXP}$: total concentration of free nucleotides, $c_{GXP} = c_{GTP} + c_{GDP}$. $g$: parameter controlling the influence of oligomers and inactive dimers on the nucleation and catastrophe rate constants

introducting an extra mechanism that helps to synchronize the MTs. Therefore, we modified the functional expressions for nucleation and catastrophe, allowing for some influence of oligomers and TU · GDP. Technically, this is achieved by replacement of the TU · GTP concentration, $c_{act}$, by an effective concentration, $c_{eff}$, which can be understood as $c_{act}$ diminished by the existence of oligomers and TU · GDP. The parameter $g$ in the formula for $c_{eff}$ defines how much the effective concentration is reduced by oligomers and TU · GDP. If $g=0$, we have the "classical" situation (no reduction). The special form of the $g$-term is chosen only for practical reasons: For small $g$ values and/or small oligomer and TU · GDP concentrations ($c_{oligo}$, $c_{ina}$), $c_{eff}$ is nearly linear in $c_{oligo}$ and $c_{ina}$.

*Rescue*

Experimental data on the rescue rate are sparse and indicate a rather weak dependence on the dimer concentration. In the model, rescue is described by an invariable rate constant, $k_{resc}$.

*Depolymerization*

For an adequate description of the total depolymerization of finite MTs, the length distribution of the S-MTs should be known. In MTOSC, MTs are measured by the concentrations of tubulin dimers incorporated in G- and S-MTs ($c_{grw}$ and $c_{shr}$, respectively) and by the corresponding MT number concentrations ($c_G$ and $c_S$). The ratio $c_{shr}/c_S$ is the mean degree of polymerization of the S-MTs. Thus, in the term describing the disappearance of S-MTs ($k_{depol} \cdot c_s^2/c_{shr}$, Eq. (2)), the length distribution can roughly be taken into account: as an approximation, the disappearance of S-MTs is assumed to be proportional to the number concentration of S-MTs, $c_S$, where the rate constant is identical with the rate of depolymerization, $k_{depol}$ (in dimers/s), scaled by the average number of dimers incorporated in S-MTs, $c_{shr}/c_S$.

The consequences of this approximation can best be visualized by considering a hypothetical solution of MTs which are all of the same length ("spike distribution") and which start shortening without rescue at the same time. The number concentration would be constant until the time when all MTs disappear simultaneously. The rate of depolymerization, $dc_{shr}/dt$ (measured in dimers/s) would also stay constant, thus leading to a linear decrease of the concentration of dimers incorporated in MTs ($c_{shr}$, in this case). According to Eqs. (2) and (3), this behavior would be approximated by a smooth, exponential decay of both the concentration of polymerized dimers, $c_{shr}$, and the MT number concentration, $c_S$. It has been shown that in the case of an exponential length distribution, the depolymerization time course is nearly exponential (Kristofferson et al. 1980).

Depending on the set of rate constants used in MTOSC, the approximative treatment of MT depolymerization may be acceptable or not. We expected it to be sufficient for extreme oscillations with phases of almost total depolymerization (like those of Fig. 2, see Results), for two reasons: Firstly, under oscillation conditions, depolymerization of MTs is so fast compared to all other processes that the exact time course of the decay of individual MTs will be unimportant. (With a depolymerization rate of 8000 dimers/s, the time for total decay of a typical MT of 20 μm length is only 4 s. This is even short compared to the time of overall depolymerization, typically 20–30 s, showing that synchrony of MTs is by no means complete.) Secondly, because of the almost total decay of MTs followed by renucleation between two cycles of polymerization, the distribution of MT lengths in subsequent maxima remains rather sharp and comparable to the first maximum. Thus, error contributions due to the approximate treatment of the depolymerization phases do not increase from cycle to cycle and error accumulation during subsequent cycles of polymerization is largely under control.

These assumptions were tested by comparison with extended systems of differential equations, MT100, MT1000, and MTSTEP (described in the Appendix), which include explicit length distributions of G- and S-MTs. The agreement between all formulations of the reaction model is excellent for oscillations with complete depolymerization, as expected, and more surprisingly, for other oscillations and normal polymerizations, differences between the solutions of MTOSC and those of the other systems are quite marginal.

*Dissolution of oligomers*

Oligomers are considered as intermediate products of MT disassembly. Dissolution of oligomers is certainly a complex process, but here it is modelled for simplicity as unidirectional first order decay with rate constant $k_{oli}$. Oligomers are believed to consist of TU · GDP only. Exchange of GDP by GTP is not possible in the oligomer state but occurs only on free dimers, after dissolution of the oligomers (Zeeberg et al. 1980).

*Nucleotide exchange*

A detailed description of nucleotide exchange should at least include the processes of association and dissociation of the $Mg^{++}$-complexes of both nucleotides. Depending on buffer conditions, $Mg^{++}$-free nucleotides should also be taken into account. We use a simplified approach, based on the following approximations, which seem to be justified at least for oscillation conditions (i.e. with 20 mM $Mg^{++}$, in large excess over the GTP concentration): (*1*) All nucleotides are complexed with $Mg^{++}$. ($c_{GTP}$ and $c_{GDP}$ denote the concentrations of free $Mg^{++}$-nucleotide complexes in the solution.) (*2*) Tubulin dimers have either $Mg^{++}$-GTP or $Mg^{++}$-GDP bound at the exchangeable nucleotide binding site (TU · GTP or TU · GDP, respectively); dimers without nucleotide are neglected. (*3*) At a given ratio $c_{GTP}$:$c_{GDP}$ the TU · GTP and TU · GDP concentrations tend to approach a ratio, $c_{act}$:$c_{ina}$, which is determined by the relative affinity, $r$, of GTP compared to GDP: $c_{act}/c_{ina}=(K_{GTP}/K_{GDP}) \cdot (c_{GTP}/c_{GDP})=r \cdot (c_{GTP}/c_{GDP})$,

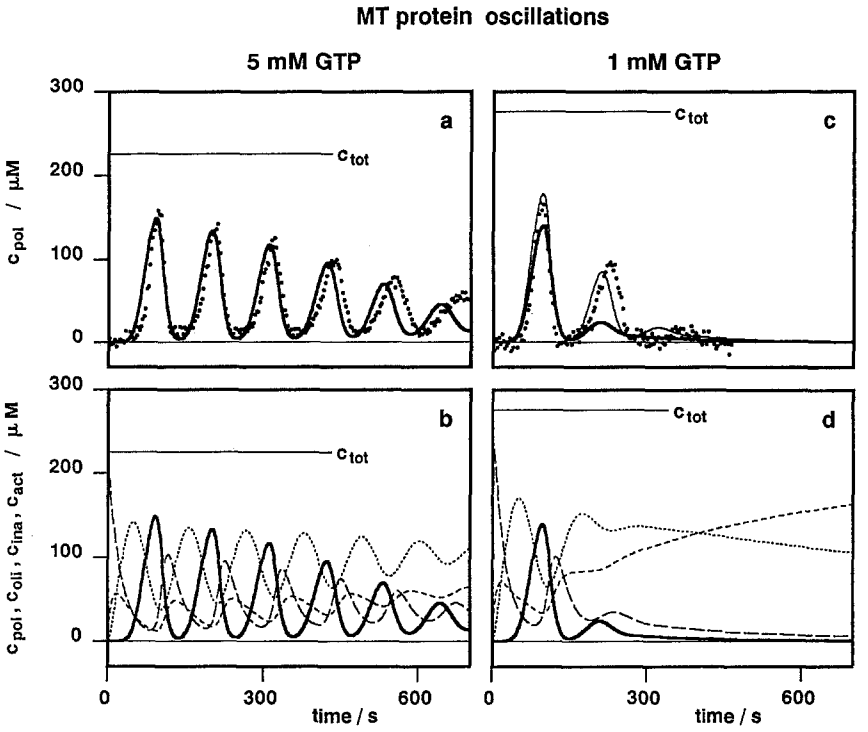


**Fig. 2a–d.** Oscillations in MT-protein solutions after a rapid temperature jump from 4 °C to 37 °C, compared to simulations by MTOSC. **a** and **b** 31 mg/ml MT-protein in oscillation buffer (100 mM PIPES at pH 6.9, 20 mM $MgCl_2$, 60 mM NaCl, 5 mM DTT) with 5 mM GTP. **c** and **d** 38 mg/ml MT-protein in oscillation buffer with 1 mM GTP. The total concentration of dimers, $c_{tot}$, is calculated on the assumption that MT-protein contains 20 weight-% MAPs. **a** and **c** Extent of polymerization determined by solution X-ray scattering (*dots*) and simulated by MTOSC (*lines*). The parameters used for calculations are compiled in Table 2. The solid line in **c** is calculated with the same parameters as used in **a**, the only difference is the change in $c_{tot}$ and the initial concentration of GTP according to the experimental conditions (no fit). Better agreement with the experiment in **c** could be realized by parameter optimizing. The thin curve in **c** has been calculated with the same parameters except for $r = 3$ (instead of 2) and with an initial GTP concentration of 1.2 mM (within the limits of uncertainty). **b** and **d** Variation of some of the other variables during the oscillations. Note that $c_{act}$ (and, hence, the amount of protein bound GTP) oscillates roughly in antiphase to $c_{pol}$. *solid line:* $c_{pol}$, extent of polymerization (as in **a** and **c**, respectively, for reference); *dotted line:* $c_{act}$, concentration of assembly competent dimers; *short dashes:* $c_{ina}$, concentration of assembly incompetent dimers; *long dashes:* $c_{oli}$, dimer equivalent concentration of oligomers

$K_{GTP}$ and $K_{GDP}$ being the equilibrium association constants for GTP and GDP, respectively (Bayley and Martin 1986). The assumption is, that the equilibrium values of $c_{act}$ and $c_{ina}$ are approached according to a single exponential relaxation mechanism, characterized by the rate constant $k_{exc}$.

An additional term for spontaneous hydrolysis of GTP, $k_{spon}\, c_{GTP}$ (Eq. (7)), was found to be useful for the quantitative simulation of X-ray data. Generally, damping of MT-oscillations in X-ray experiments is stronger than in light-scattering. Presumably, this will be a combined effect of protein damage and accelerated decomposition of GTP. It has been observed (Marx et al. 1990) that decomposition of GTP is induced by X-ray irradiation, yielding a diversity of products including GDP. The additional term in Eq. (7) accounts for these effects by increasing the concentration $c_{ina}$ of "inactive" dimers.

The differential equations were solved numerically by using the fourth-order Runge-Kutta method with adaptive step size control (Press et al. 1988). The programs for all systems (MTOSC, MT100, MT1000, MTSTEP), providing handling of model parameters and start values, numerical integration, as well as graphical and numerical output, are available upon request.

## IV. Results

### *a) Modelling of large amplitude oscillations observed by X-ray scattering*

We tried to simulate real MT oscillations, as observed in tubulin solutions by light or X-ray scattering at high protein concentrations with $Mg^{++}$ in excess of GTP. Figure 2a (dots) shows an example for particularly strong oscillations in a solution of MT-protein containing 5 mM GTP. Figure 2c (dots) shows the result of a similar experiment with only 1 mM GTP and slightly different tubulin concentration. Both experiments are quite similar with regard to the lag-time before the onset of polymerization, the form of the first polymerization peak and the nearly total disassembly of MTs in the minima. The main difference comes from strong damping of the oscillation in Fig. 2c, obviously related to GTP-depletion. The oscillation of Fig. 2a was used as the main reference for model calculations because MTs apparently are highly synchronized as judged by the virtual absence of MTs in the minima.

On the basis of the dynamic instability of single MTs, synchrony of the whole MT population is considered to

**Table 2.** Parameters used in numerical simulations and comparison with experimental data

| | Units | Simulations | | | Experiments | |
|---|---|---|---|---|---|---|
| | | MT-prot., osc. buff. (Fig. 2) | PC-tubulin, osc. buff. (Fig. 3a) | PC-tubulin, reass. b. (Fig. 3b) | plus ends | minus ends |
| $k_+$ | $\mu M^{-1} s^{-1}$ | 15 | 15 | 10 | 7 (11)[b] | 4 (5)[b] |
| $k_-$ | $s^{-1}$ | 120 | 120 | 45 | 43 (89)[b] | 25 (33)[b] |
| $k_{depol}$ | $s^{-1}$ | 8000 | 8000 | 800 | 800 (8000)[b] | 840 (8000)[b] |
| $q_{cat}$ | $s^{-1}$ | 0.00015 | 0.00015 | 0.00008 | -- | -- |
| $z_{cat}$ | $\mu M$ | 80 | 80 | 80 | -- | -- |
| $s_{cat}$ | $\mu M$ | 10 | 10 | 10 | 4–13[c] | 4–13[c] |
| $k_{resc}$ | $s^{-1}$ | 0.2 | 0.2 | 0.4 | 0.08 (0.09)[b] | 0.36 (0.17)[b] |
| $g$ | $\mu M^{-1}$ | 0.021 | 0.008 | 0.008 | -- | -- |
| $q_{nuc}$ | $\mu M^{-1} s^{-1}$ | 0.00012 | 0.00012 | 0.00012 | -- | |
| $z_{nuc}$ | $\mu M$ | 60 | 60 | 60 | -- | |
| $s_{nuc}$ | $\mu M$ | 60 | 60 | 60 | -- | |
| $k_{oligo}$ | $s^{-1}$ | 0.04 | 0.04 | 4[a] | $\approx 0.02$[d] | |
| $k_{exc}$ | $s^{-1}$ | 0.08 | 0.08 | 0.08 | 0.1–0.2[e] | |
| $r$ | 1 | 2 | 2 | 2 | 1.9–2.5[f] | |
| $k_{spon}$ | $s^{-1}$ | 0.0003 | 0.001 | 0.001 | -- | |

[a] Oligomers are discarded from the reaction cycle by choosing a very high dissociation rate
[b] Obermann-Pleß (1992); results obtained by dark-field microscopy of single MTs at tubulin concentrations in the range from 1.3 to 3.8 mg/ml. Values in parentheses are measured in oscillation buffer (0.1 M PIPES pH 6.9, containing 4 mM GTP, 20 mM $MgCl_2$, and 60 mM NaCl), other values in standard reassembly buffer (0.1 M PIPES pH 6.9, containing 1 mM GTP and 1 mM $MgSO_4$)
[c] Walker et al. (1988, 1991)
[d] Melki et al. (1988, 1989); the rate depends on buffer conditions (e.g. concentration of $Mg^{++}$) and protein composition (MAPs)
[e] Engelborghs and Eccleston (1982); Melki et al. (1988, 1989)
[f] Martin and Bayley (1987)

be a consequence of the nonlinear dependence of catastrophe and nucleation/rescue on the TU · GTP concentration. It has been demonstrated by model calculations that such nonlinearities can provoke oscillations (Carlier et al. 1987; Chen and Hill 1987; Lange et al. 1988; Bayley et al. 1989), but the simulations were quite different from real MT oscillations. One could argue that better agreement can be obtained by optimizing the model without changing the basic assumptions. To see if this is true, we reformulated the reaction cycle (see Theory and Table 1) and tried to avoid oversimplifications in order to get realistic simulations.

The curves shown in Fig. 2 are results obtained by numerical integration of the MTOSC system of equations given in Table 1. The parameters are listed in Table 2, together with experimental values from the literature. The solid lines in Fig. 2a, c have been calculated with the same set of parameters except for the initial concentrations of tubulin and GTP. Better agreement between calculations and real oscillations can be obtained if the parameters for both oscillations are fitted independently (thin line in Fig. 2c).

However, special assumptions about catastrophe and nucleation have been introduced in order to generate the simulations shown in Fig. 2. With the usual assumption that the catastrophe and nucleation rates depend on the concentration of TU · GTP only, the model cannot reproduce the typical form of real oscillations. Similar to the results of other authors (Carlier et al. 1987; Chen and Hill 1987; Lange et al. 1988; Bayley et al. 1989), either smooth oscillations with incomplete depolymerization or oscillations with almost total depolymerization but untypical, sawtooth-like shape were obtained. For realistic simulations, either the assumptions on dynamic instability must be changed or another mechanism for better synchronization of the MTs must be introduced. Some possible mechanisms will be considered below (see Discussion). To be specific, we assumed that the catastrophe rate is increased by the presence of oligomers and/or TU · GDP. This is achieved by using an "effective concentration" $c_{eff}$ instead of the TU · GTP concentration $c_{act}$ as argument of the catastrophe rate constant (see Table 1 and Theory). With this modification of the catastrophe term, the model can simulate strong oscillations with deep depolymerization. For best fits with real oscillations, the nucleation term was also modified by replacing $c_{act}$ with $c_{eff}$. If oligomers or TU · GDP can induce disassembly of marginally stable MTs (see Discussion), it seems plausible that nucleation may also be affected.

### *b) Simulation of less pronounced oscillations*

In the "standard formulation" of our model ("MTOSC", see Table 1 and Theory), the distribution of MT lengths is not considered in detail. The mean length of the MTs is the only parameter related to the length distribution which is used implicitly in Eq. (2) of MTOSC. By comparison with the results of calculations with explicit length distributions (see Appendix), the approximation by MTOSC was found to be highly satisfactory for large

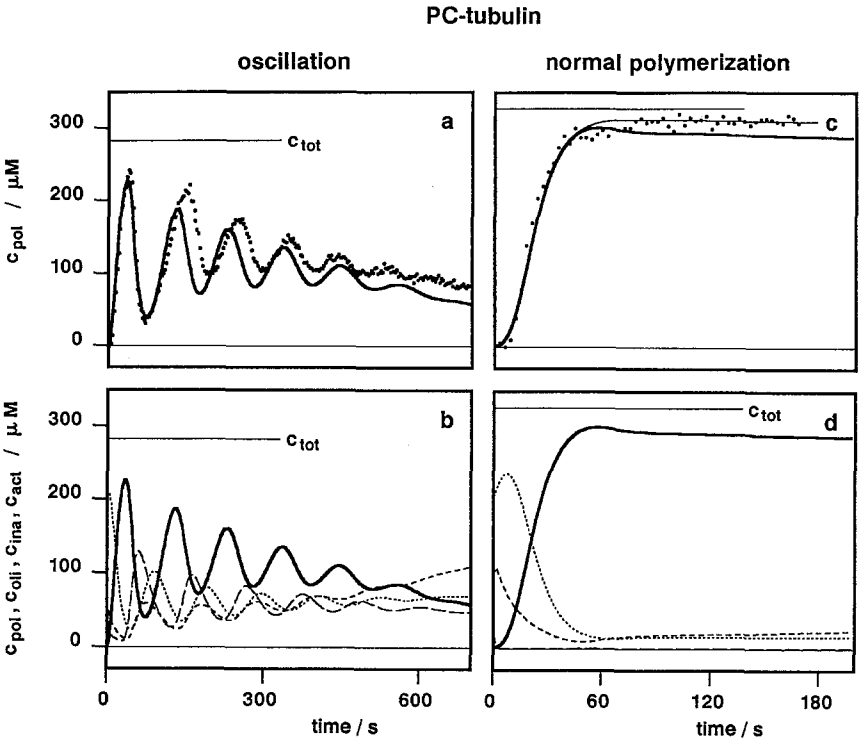


**Fig. 3.** Oscillation and normal polymerization in PC-tubulin solutions, compared to simulations by MTOSC. **a** and **b** 31 mg/ml PC-tubulin in oscillation buffer (100 mM PIPES at pH 6.9, 20 mM $MgCl_2$, 60 mM NaCl, 1 mM DTT) with 7 mM GTP. **c** and **d** 36 mg/ml PC-tubulin in reassembly buffer (100 mM PIPES at pH 6.9, 1 mM DTT) with 2 mM GTP and 2 mM $MgCl_2$. **a** and **c** Extent of polymerization determined by solution X-ray scattering (*dots*) and simulated by MTOSC (*lines*). The parameters used for calculations are compiled in Table 2. The simulations shown in **a** (PC-tubulin oscillation) and that shown in Fig. 2 (MT-protein oscillation) differ mainly by the parameter $g$, which describes the influence of oligomers and TU · GDP on nucleation and catastrophe: for PC-tubulin, $g$ is reduced to 0.008 compared to 0.021 for MT-protein. Other changes concern $c_{tot}$ and the initial GTP concentration (experimental constraints) and the rate of spontaneous GTP hydrolysis, which determines the damping rate of the oscillations. The solid line in **c** is the result of a simulation with parameters taken from the simulation in **a** and changed according to the experimental results obtained by microscopic observation of single MTs (see Table 2). The most important change is the reduction of $k_{depol}$, the rate of depolymerization, by a factor of 10. Furthermore, oligomers are eliminated from the reaction cycle by a drastic increase of the decay rate, $k_{oligo}$. The overshoot seen in the simulation (*thick curve*) is not unusual for normal polymerizations. A better fit to the experimental data is possible if the parameters are considered to be free. For instance, increasing $s_{cat}$ from 10 µM to 13 µM results in the monotonic polymerization shown by the thin line. **b** and **d** Variation of some of the other variables according to the simulations of **a** and **b**; same symbols as in Fig. 2. Note that $c_{act}$ (and, hence, the amount of protein bound GTP) oscillates roughly in antiphase to $c_{pol}$

amplitude oscillations such as those in Fig. 2: Since each polymerization peak is followed by almost complete disassembly and renucleation, length distributions remain confined to a rather narrow range. For oscillations with incomplete depolymerization phases, deviations between the different calculations were expected to be larger. However, in most cases the correspondence was surprisingly close. Figure 3a shows an example of incomplete oscillations, measured by X-ray scattering, and a simulation by MTOCS. In Fig. 4, the same simulation is compared with the results of various calculations including explicit length distributions. The main point is that introduction of explicit length distributions does not change the results appreciably.

### *c) Transition from oscillations to monotonic polymerization*

Calculations with explicit length distributions showed that the MTOSC system can be used to describe oscillations as well as normal polymerization. Now we address the question of whether the striking difference in polymerization behavior observed in standard and oscillation buffers can be attributed to changes in the dynamic instability parameters as determined by video microscopy.

Figure 3c shows the result of an experiment with PC-tubulin as in 3a, but in standard reassembly buffer (2 mM GTP, 2 mM $MgCl_2$). The thick curve in panel c has been calculated with the same parameters as the curve shown in panel a, with the following exceptions: firstly, the rate of rapid depolymerization, $k_{depol}$, is reduced by a factor of 10, the catastrophe rate is reduced by a factor of 2, and the rates of dimer association and dissociation in the growing state, $k_+$ and $k_-$, are diminished from 15 $\mu M^{-1} s^{-1}$ to 10 $\mu M^{-1} s^{-1}$ and from 120 $s^{-1}$ to 60 $s^{-1}$, according to the results obtained by video-microscopy (see Table 2). Secondly, it is assumed that oligomers play a minor role in standard reassembly buffer. Without change of the equations, this is accomplished by using a very high rate of oligomer dissolution, $k_{oligo}$. Within the MTOSC model (with $g > 0$), the presence of oligomers has a twofold effect

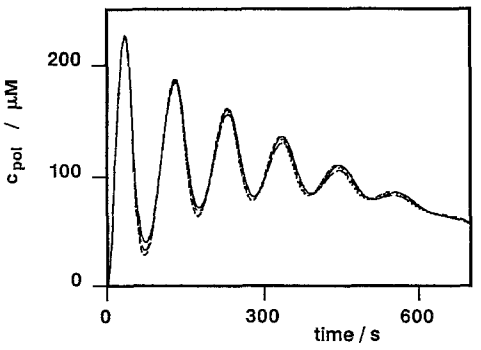


**Fig. 4.** Extent of polymerization, $c_{pol}$, calculated according to MTOSC (*continuous line*), MT100 (*long dashes*), MT1000 (*short dashes*), and MTSTEP (*dotted line*). The results of MT1000 and MTSTEP are virtually identical. Parameters are the same as in Fig. 3a, b. (*Computing times:* MTOSC (7 Eq.): 10 s; MT100 (209 Eq.) 44 s; MT1000 (2009 Eq.): 1838 s; MTSTEP (2010 Eq.): 3621 s; IMB compatible PC with INTEL i486 processor, 33 MHz)

on polymerization: (*1*) Oligomers contribute to the synchronization of the MTs via their effect on catastrophe and nucleation. (*2*) Oligomers play an important role as an intermediate storage form of inactive dimers. The regeneration of assembly competent TU · GTP is delayed by slow dissolution of oligomers. The retardation of TU · GTP regeneration from disassembling MTs is essential for the synchronization of MTs (Carlier et al. 1987; Mandelkow et al. 1988; Melki et al. 1988). Conversely, when oligomers are absent, dimer recycling is faster and as a consequence, oscillations are more difficult.

Reducing the depolymerization rate has also two effects on the characteristics of MT polymerization; besides the direct effect of slowing down the depolymerization, the contribution of rescue events becomes more important. Even if the rescue rate is the same in oscillation and standard reassembly buffer, the percentages of S-MTs which are rescued before total disassembly can be quite different as the number of rescue events depends on the rescue rate *and* the duration of shortening.

## V. Discussion

Previous attempts to explain oscillations by mathematical models based on the dynamic instability were only partially successful: It could be shown that nonlinearities in catastrophe, rescue, and nucleation in combination with slow regeneration of assembly competent dimers produce oscillations, but all model curves presented so far were quite different from real oscillations. Discrepancies between measured and calculated oscillations could be explained either by problems in the mathematical formulation of the reaction mechanism, or by deficiencies in the reaction mechanism itself. If there are deficiencies in the reaction mechanism, one might ask whether these are fundamental for the understanding of MT dynamics or not.

In order to clarify these questions, we tried to develop a simple but still realistic formulation, starting from usual assumptions on the reaction mechanism. In our approach, the reaction cycle is described by a set of differential equations which is solved by numerical integration. In previous model calculations using a similar approach (Carlier et al. 1987), serious restrictions were imposed on the reaction model, because depolymerization and total decay of MTs cannot be described straightforwardly by differential equations. For a rigorous treatment, time-consuming Monte-Carlo calculations seemed to be inevitable (Carlier et al. 1987; Chen and Hill 1987; Bayley et al. 1989). However, we found simple approximations at various degrees of accuracy (see Theory and Appendix) which turned out to be very useful.

The main conclusion from our model calculations is a negative one: the nonlinear dependence of catastrophe and nucleation/rescue on the TU · GTP concentration is *not sufficient* to explain real MT oscillations. Thus, either the "short cap hypothesis" (i.e. the assumption that transition rates depend only on the current values of the concentration variables; see Introduction) must be abandoned, or the reaction cycle must be completed by introducing a mechanism which promotes self-synchronization of the MTs. In the following part of the discussion we will deal with possible objections against this conclusion.

### *a) Need for a special synchronization mechanism: pros and cons*

Only the most important phenomena, considered to be essential for MT-oscillations, are included in the MTOSC model. For example, the difference between plus and minus ends is ignored, as well as breakage and annealing of MTs (Rothwell et al. 1987) and any variability in the structure (e.g. varying protofilament numbers, Chretien et al. 1992) and the dynamics of MTs (variable rates of growth and shortening, Gildersleeve et al. 1992). Of course, this renders the model less realistic. However, with all these effects included, synchrony of the MT population would decay even more rapidly than predicted by the simple model. Hence, the failure of the original model (Table 1 with $g=0$) to explain smooth oscillations of large amplitudes makes the need of significant modifications even more obvious.

It is evident from Fig. 2 that large amplitude oscillations cannot be described by assuming a fixed number of MTs and thereby avoiding the problems of dealing with nucleation and complete disassembly of MTs. As the natural assumption, a power-law ($k_{nuc} \sim [\text{TU} \cdot \text{GTP}]^n$) is sometimes used to describe the dependence of the nucleation rate on the concentration of polymerization competent dimers. This implies that nucleation is rate-limited by an elementary process of order $n$. However, the creation of a nucleus seems to involve a more complex sequence of reaction steps (Voter and Erickson 1984). So, with regard to our finding that the special form of the TU · GTP-dependence does not affect the main conclusions (see below), it seems that one may approximate nucleation by an exponential function of the TU · GTP concentration.

If dimer association and dissociation were the relevant processes for both the growing and the shortening state a

steep TU · GTP-dependence would be expected for catastrophe as well as for rescue (cf. Bayley et al. 1990). However, kinetic studies of MT solutions using small angle X-ray scattering (Lange et al. 1988) and time-resolved cryo-electron microscopy (Mandelkow et al. 1991) indicate that MTs disassemble by falling apart into oligomers, at least in oscillation buffer or in the presence of MAPs. Accordingly, no significant variation of the rescue rate constant, $k_{resc}$, could be detected within the narrow range of TU · GTP concentrations available to microscopic observation of single MTs (O'Brien et al. 1990; Trinczek et al. 1993). Moreover, for the oscillations in Fig. 2, rescue seems to play a minor role, if any. Therefore, in our model we consider $k_{resc}$ to be constant. As the main effect of rescue is to advance the termination of the depolymerization phase, rescue was usually neglected in attempts to generate deep depolymerization without hysteresis (see below).

At first sight, the failure of the unmodified system to simulate real oscillations seems to be a problem of (*i*) finding an appropriate set of kinetic parameters and (*ii*) finding better descriptions for the TU · GTP-concentration dependences of the catastrophe and nucleation rate constants.

(*i*) In spite of the high number of parameters (12 independent kinetic parameters, without $g$; see Table 1), the range of acceptable parameter sets is rather limited, because of the restrictions imposed by the rate constants that have been determined experimentally. Although one has to allow some difference between experimental values and the values used in simulations (e.g. because of uncertainties in experimental rate constants, differences in preparations, and for compensation of neglected effects like MT polarity, annealing and others) it seems unlikely that we missed the optimum set of parameters because it is located in a totally different region of parameter space.
(*ii*) Catastrophe and nucleation rate constants should be continuous and monotonic functions of the TU · GTP concentration, and they should have threshold-like characteristics. The important features of candidate functions are the threshold value and the sharpness of the transition from negligible to highly effective rates. In the exponential relationship we use, the threshold value is determined by $z$ and the sharpness by $s$ (at fixed scale factor $q$; see Table 1). For the question of whether or not smooth oscillations with deep depolymerization are possible, the exact shape is of minor significance. This has been found by a large number of trials with various functional forms. The following considerations will make this plausible.

When the concentration of TU · GTP has dropped due to MT polymerization and reached the "catastrophe threshold", MTs switch to the shortening state with a certain degree of synchrony. Synchrony can never be 100% as long as catastrophe events occur at a finite rate. Why is it not possible to attain any desired degree of synchrony just be making the rate function steep enough? The reason is that even at the top of polymerization (maximum extent is ca. 70% of the total tubulin), the concentration of TU · GTP is regulated by consumption (by growing MTs) and production (from inactive protein in the form of oligomers and TU · GDP). When consumption decreases abruptly, because part of the MTs switch to shortening, the TU · GTP concentration goes up immediately. Hence, catastrophe stops too early, even if the rate function is extremely steep: If a function changes rapidly upon small changes of its argument, this is true (with opposite signs) for both directions, increasing and decreasing arguments.

An obvious solution of the problem would be the assumption of hysteresis in the catastrophe rate: once the catastrophe region has been entered, the catastrophe rate remains at a high level, even if the TU · GTP concentration increases again. This implies that the catastrophe rate is not longer a unique function of the TU · GTP concentration. The most natural explanation for hysteresis-like catastrophe is the assumption that MTs are destabilized by their disassembly products (oligomers and/or TU · GDP). This is incorporated in the MTOSC model by replacing the TU · GTP concentration in the argument of the catastrophe rate function with an "effective" concentration, which is the TU · GTP concentration reduced owing to the presence of oligomers and TU · GDP (see Table 1, Theory).

The form that we use for describing MT destabilization by disassembly products may be arbitrary to a certain extent. We deliberately chose the formulation involving an effective concentration $c_{eff}$ of assembly competent dimers because it avoids major changes in the whole set of equations, and because it does not refer specifically to dynamic instability models. So, the same formulation could also be interpreted as an approximative description of other possible synchronization mechanism (see below). For instance, in case of direct co-operativity between MTs, the introduction of $c_{eff}$ should be considered as a (special) way to account for hysteresis in the catastrophe rate. If MT synchronization results from co-operative effects in TU · GTP regeneration (for instance, from temporary depression of the dimer concentration caused by oligomer release) $c_{eff}$ could be closer to the true TU · GTP concentration than the nominal concentration $c_{act}$.

### *b) Possible sources of synchrony*

In this section we discuss some possible mechanisms that could help to maintain a high level of synchrony within the MT population.

*Extended cap models.* According to the extended cap model, the E-site nucleotide is not hydrolysed immediately after incorporation of the TU · GTP dimer but hydrolysis is somewhat delayed. As a result, a stabilizing region of TU · GTP dimers appears at the end of a growing MT. The length of the GTP-cap varies with the growth velocity. Catastrophe occurs whenever the GTP-cap shrinks to zero. Hence, the probability for catastrophe is low at high TU · GTP concentrations (i.e. high growth rates). It increases with decreasing TU · GTP concentration, but it depends also on the growth history of the MT's.

Several rules of hydrolysis have been considered (see Stewart et al. 1990; Walker et al. 1991; Erickson and

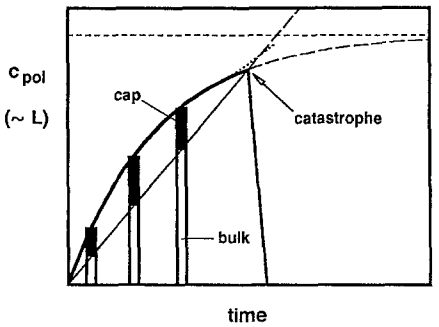


**Fig. 5.** A cycle of polymerization and depolymerization according to a hypothetical extended cap model: All MTs nucleate at time $t=0$ and grow from a given pool of assembly competent dimers. Without catastrophe, the extent of polymerization, $c_{pol}$, approaches $c_{tot}-c_{crit}$ ($c_{tot}$: total concentration of dimers, $c_{crit}$: critical concentration of elongation), following an exponential time course. The interface between the stable cap (black) and the unstable core (white) proceeds at constant velocity ("vectorial hydrolysis", Stewart et al. 1990). At the beginning, polymerization is faster than propagation of the interface, and the caps grow longer and longer. Later on, when polymerization slows down, the caps shrink. For three arbitrary time points, the state of the MTs is represented schematically. When the caps disappear, MTs switch to rapid shortening. Without furher effects, repetition of these processes results in sawtooth-like oscillations. In the Lateral Cap model, the probability for catastrophe is determined by the momentary value of $c_{act}$. Catastrophic transition of the total ensemble of MTs cannot be attained because $c_{act}$ itself reacts to catastrophe (negative feedback, see Discussion). In the vectorial cap model, depolymerization of all MTs is more likely: It is not necessary that all MTs switch to shortening at the same time. Even if elongation of late MTs is accelerated as a consequence of the decomposition of early MTs (as indicated by the dotted line), they have little chance to escape once and for all

O'Brien 1992). In Fig. 5, the uncoupled vectorial hydrolysis model is used to illustrate how large amplitude oscillations can be explained, in principle, by an extended GTP-cap model. Figure 5 shows the fate of a MT which may be considered as representative of the whole population of MTs growing from a pool of assembly competent dimers (for details see legend to Fig. 5). In previous simulations of MT oscillations (including those presented by Carlier et al. 1987), catastrophe was assumed to occur when the concentration of free dimers approaches a critical lower limit or, in other words, when a certain extent of polymerization is reached. In the case of a single MT (no rescue) this would obviously result in total depolymerization. However, as discussed above, a large population of MTs would never depolymerize completely under realistic conditions because catastrophic transitions occur stochastically within a certain time span: depolymerization of early MTs will reduce the transition probability for late MTs via their effect on the concentration of free subunits (negative feedback!). In the vectorial cap model as illustrated by Fig. 5, the time point of catastrophe is determined by the internal state of the MT. Both, the stochastic character and the sensitivity to changes in the TU · GTP concentration are largely reduced: even a rise in the TU · GTP concentration due to the decay of early MTs (dotted line) does not prevent catastrophic decay of the other MTs unless the rise is very pronounced.

Experiments suggest that the caps must be short, possibly restricted to the terminal layer of dimers (Stewart et al. 1990; Walker et al. 1991; Voter et al. 1991). Short caps, however, seem not to be able to provide sufficient time delay to explain high amplitude oscillations. Moreover, there is an essential difference between the MTOSC model and any model based on extended caps: Extended caps could only reduce the speed of desynchronization. It is unlikely that under real conditions (with all the desynchronizing effects that we neglected), this is sufficient to explain oscillations with phases of complete depolymerization. In contrast, a positive feedback mechanism as used in the MTOSC model (disassembly of MTs induced by the products of disassembly, for instance) could even explain spontaneous synchronization.

*Destabilization of MTs by disassembly products.* Our calculations show that high amplitude oscillations like those in Fig. 2 can be generated if one assumes that oligomers and/or TU · GDP induce catastrophe in growing MTs. The concept of marginally stable MTs makes this assumption more plausible. From the structural point of view, marginally stable MTs are characterized by an incomplete cap (c.f. Bayley et al. 1990), most probably combined with conformational irregularities at the ends (see Fig. 6a). Kinetically, marginal stability can be described as an intermediate state between the extremes of growth and shortening with high probabilities for transitions to either growth or shortening. In oscillations, the number of marginally stable MTs will be highest at the maxima of the extent of polymerization.

*Destabilization by oligomers.* MTs are supposed to be under mechanical stress because the MT core consists of TU · GDP, and protofilaments of TU · GDP tend to assume an intrinsic curvature (Howard and Timasheff 1986; Melki et al. 1989; Mandelkow et al. 1991; Erickson and O'Brien 1992). The energy released by protofilaments coiling off the MT overcompensates for the breakage of lateral bonds, and the surplus energy can be used for mechanical work like the movement of chromosomes (Koshland et al. 1988; Coue et al. 1991). Protofilament coiling will most probably start at the end of an intact MT; otherwise longitudinal bonds must be broken before curling is possible. In growing MTs, stabilizing caps prevent depolymerization from the ends. Since oligomers are curled pieces of protofilaments, they could associate laterally to MTs and especially to the ends of marginally stable MTs. Interactions between protofilaments and oligomers will be competitive with the normal inter-protofilament interactions and may force MTs to undergo catastrophic transitions (Fig. 6b).

*Destabilization by TU · GDP.* According to the Lateral Cap model, the catastrophe rate depends on fluctuations of a small GTP-cap restricted to the terminal layer of dimers. By Monte Carlo numerical simulation, Bayley et al. (1990) demonstrated that the catastrophe rate is a nonlinear function of the free TU · GTP concentration. It seems very likely that the presence of free TU · GDP could provoke a significant increase of the catastrophe

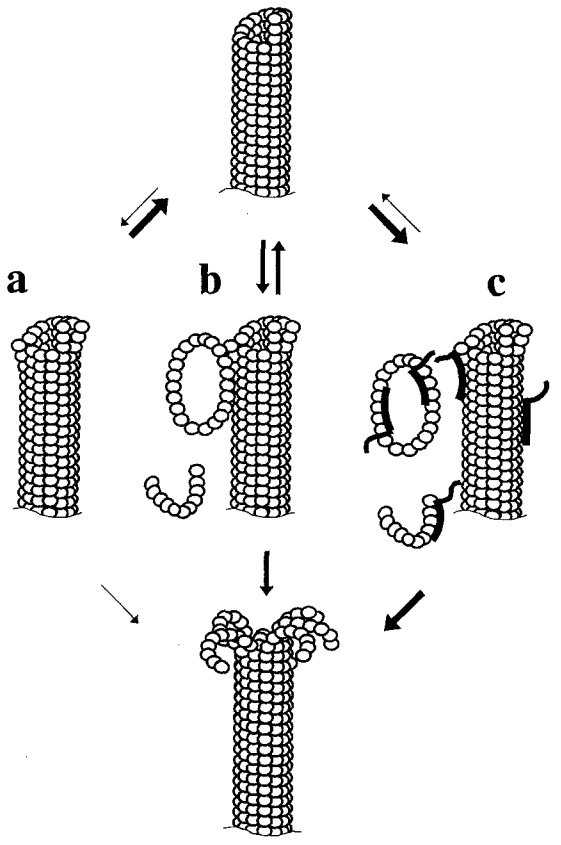


**Fig. 6a–c.** Illustration of a hypothetical mechanism for indirect interaction of MTs: destabilization of marginally stable MTs by oligomers. At the top, a stable MT is shown, which is ready to grow by association of GTP-dimers. Because of the hydrolysis of GTP to GDP, the bulk of the MT contains mainly TU · GDP. Protofilaments consisting of TU · GDP have a propensity to assume a coiled conformation. This is suppressed by a stabilizing cap (presumably a crown of TU · GTP). At the bottom, a MT in the phase of rapid shortening is shown. It depolymerizes by splitting off oligomers (curved fragments of protofilaments), some of them may form closed rings. Oligomers dissociate into TU · GDP at various rates, depending on buffer conditions and protein composition: high $Mg^{++}$ concentrations (Howard and Timasheff 1986) as well as the presence of MAPs (Melki et al. 1989) favour the formation of oligomers. **a** Intermediate states not too far from the stable state will be called "marginally stable" as long as the probability for return to normal growth is higher than the probability for transition to rapid shortening. Marginally stable MTs are represented with protofilaments slightly bent from the straight conformation. The assumption of conformational alterations at the ends of marginally stable MTs seems most adequate for the "conformational cap" hypothesis, but may also hold for the more usual GTP-cap hypothesis since nucleotide hydrolysis is known to be coupled to the equilibrium conformation of unstrained protofilaments. **b** In the presence of oligomers, the probability for transitions from the marginally stable state to the growing state is reduced by the lateral interaction between oligomers and MTs. In this way, transitions to rapid shortening are favoured. This situation may be relevant for PC-tubulin solutions in oscillation buffer (high concentration of $MG^{++}$). **c** In the presence of MAPs, the effect of oligomers on marginally stable MTs may be amplified because MAPs increase the radius of interaction and/or strengthen the interaction of MTs and oligomers

rate, provided that the probability for association of TU · GDP to MT ends is non-zero. This is confirmed by recent Monte Carlo calculations that have included the possibility of TU · GDP binding to MT ends (Martin et al. 1993). These calculations show that a relatively small fraction of TU · GDP in coexistence with TU · GTP could have large effects on MT behavior. Whilst the experimental evidence for TU · GDP supporting MT elongation has been a matter of debate for a long time, it now seems sure that TU · GDP can indeed be incorporated during copolymerization with TU · GTP (Bayley and Manser 1985; Hamel et al. 1986; Lin and Hamel 1987; Hyman et al. 1992).

*Other mechanisms for MT synchronization.* Direct interactions of MTs would be the simplest explanation for co-ordinated depolymerization. Such interactions can produce remarkable effects as indicated by the spontaneous formation of spatial patterns with MT bundling (at high protein concentrations in oscillation buffer; Mandelkow et al. 1989) or nematic liquid-crystalline ordering of MTs (at tubulin concentrations of a few mg/ml; Hitt et al. 1990; Somers and Engelborghs 1990; Tabony and Job 1990, 1992). However, it is not clear if these interactions affect the transition behavior of dynamically unstable MTs. Therefore, we prefer the assumption of indirect interactions, mediated by oligomers and/or TU · GDP. The source of synchronization could also be hidden in the complex process of TU · GTP regeneration from disassembling MTs. The MTOSC model assumes that oligomer decay and nucleotide exchange follow simple exponential relaxations. Presumably, MTs could also be synchronized by co-operativity at the oligomer or dimer level: if, for instance, oligomers act as tubulin scavengers under special conditions, then a sudden rise of the oligomer concentration by disassembly of MTs could result in a temporary decrease of the TU · GTP concentration, thus providing the positive feedback required for MT sychronization.

### *c) General implications*

Normal polymerization in tubulin solutions is characterized by a monotonic increase of the extent of polymerization. The rate of overall MT-assembly is the product of the MT number concentration and the net elongation rate. Thus, the kinetic parameters which directly influence the MT-assembly rate are the nucleation rate, $k_{nuc}$, and the on- and off-rates of MT elongation, $k_+$ and $k_-$. To study the influence of these parameters, we calculated assembly curves for various values of $q_{nuc}$ with all the other parameters held constant, and similarly, for various values of $k_+$.

Increasing the rate of nucleation by a factor of 100 (by changing $q_{nuc}$) results in only five times more MTs. Consequently, the rate of MT assembly also increases by only a factor of five. The reason is, that the gain in the nucleation rate is partially compensated by a reduction in nucleation time (i.e. the time segment at which the TU · GTP concentration is favorable for nucleation). Similarly, a 100-

fold rise of the elongation rate constant, $k_+$, results in about 25 times fewer MTs, and the MT-assembly velocity increases only by a factor of about four. Obviously, the number concentration is more influenced by the elongation rate than by the nucleation rate. In usual kinetic experiments on MT polymerization in bulk solutions, the supply of assembly competent dimers seems to be the most important factor that determines the velocity of overall MT assembly. These examples and similar calculations concerning catastrophe and MT-disassembly, show that the direct effects may be dominated by indirect but more important ones.

*Oscillation period.* If the velocity of polymerization were controlled by $k_{nuc}$ and $k_+$, and if the speed of depolymerization were controlled by $k_{cat}$ and $k_{depol}$, then the period would be determined by these parameters. Now, in general, processes such as nucleation and phase transitions are very sensitive to the experimental conditions. Hence, the period should vary in a wide range, dependent on buffer conditions, presence or absence of MAPs, temperature etc. However, the period is surprisingly constant in most cases (Obermann et al. 1990). This can be understood as an effect of auto-regulation due to the negative feed back in the original reaction cycle. In agreement with Melki et al. (1988), we find that the period of the oscillations is mainly determined by production and regeneration of TU · GTP (i.e. by $k_{oligo}$, $k_{exc}$). This lends additional support to our claim that the exact form of the nucleation and catastrophe functions, $k_{nuc}$ and $k_{cat}$, is of minor significance.

*Lag-phase.* The onset of MT-assembly is preceded by a more or less extended prenucleation period (Spann et al. 1987). This lag-phase is particularly long for MT-protein in oscillation buffer (c.f. Fig. 2 a and 3 a). According to our calculations, the number concentration oscillates nearly in phase with the extent of polymerization. The lag results mainly from suppression of nucleation by oligomers and TU · GDP: as discussed in Sect. IV (Results), we assume that the nucleation efficiency is reduced by oligomers and TU · GDP in the same way as the catastrophe rate. If we use the term "nucleus" for any minimal aggregate of dimers that just grows like a MT, then nuclei are characterized by the same kinetic properties that we used to define marginally stable MTs. Thus, it seems only consistent to assume that nucleation and catastrophe are affected by the same factors and in a very similar way.

## VI. Conclusion

We presented a simple mathematical model of tubulin polymerization kinetics, MTOSC, which can generate quantitative simulations of MT oscillations as observed by small angle X-ray solution scattering. The model is based on the reaction cycle described earlier (Mandelkow et al. 1988) comprising nucleation and growth of MTs, catastrophe and rapid shortening, slow decay of oligomers into TU · GDP and regeneration of TU · GTP from TU · GDP. The correct treatment of MT shortening requires the knowledge of MT length distributions which in turn depend on the whole history of the system. This problem has been overcome by an approximative description of MT decay, allowing considerable simplifications in the mathematical formalism. The validity of this approximation has been tested by comparison with calculations including length distributions at various degrees of accuracy (MT100, MT1000, MTSTEP). These more extensive formulations can be used, instead of MTOSC, whenever the kinetics of MT length distributions is of concern.

We found that the nonlinear TU · GTP-dependence of catastrophe and nucleation, in combination with slow regeneration of TU · GTP, is apparently not sufficient by itself to explain smooth, large-scale oscillations as observed by scattering experiments. Thus, another mechanism must help to overcome the desynchronization tendencies. In principle an extended cap model could explain real oscillation by introducing time delay into the equations of the model. However, since experimental evidence seems to be against the extended cap hypothesis, we assumed a special feedback mechanism for MT synchronization. As a candidate mechanism we propose the destabilization of MTs by disassembly products, implying the ability of oligomers and/or TU · GDP dimers to interact with the ends of MTs.

*Acknowledgements.* We thank M. Koch and the staff of EMBL-Hamburg for making their X-ray facilities available. We are grateful to E.-M. Mandelkow, H. Obermann-Pleß, and B. Trinczek for valuable discussions. We thank P. M. Bayley for many helpful comments. This project was supported by the Deutsche Forschungsgemeinschaft and the Bundesministerium für Forschung und Technologie.

## Appendix

For a correct treatment of MT disassembly, it is necessary to consider the distributions of MT lengths. In the MTOSC formulation of the reaction cycle, this is roughly accomplished by relating the rate of disappearance of *S*-MTs to the average length of these MTs. In order to test this approximation, we expanded the MTOSC system by introducing explicit length distributions for *G*- and *S*-MTs.

### *First expansion of the MTOSC model: MT100*

In the MT100 system of differential equations (Table 3), the quasi-continuous length distributions of G- and S-MTs are approximated by discrete distributions, considering 100 different lengths from $1 \cdot p$ μm to $100 \cdot p$ μm in steps of $p$ μm ($p$ is a positive, real number, typically in the range between 0.5 and 5). The number concentrations of MTs of these lengths (intermediate lengths have to be rounded) are used as additional variables. Thus, $c_G^i$ and $c_S^i$ are the number concentrations of $i \cdot p$ μm long *G*- and *S*-MTs, respectively ($i = 1, 2, \ldots, 100$). The time derivatives of these variables extend the system of differential equations by 200 equations. An additional variable, $c_G^0$, is in-

**Table 3.** MT100 system of differential equations

$$
\begin{aligned}
\dot{c}_G^0 &= k_{\text{nuc}} && && -\frac{k_+ c_{\text{act}} - k_-}{p\,1625} c_G^0 \\
\dot{c}_G^i &= -k_{\text{cat}} c_G^i && +k_{\text{resc}} c_S^i && +\frac{k_+ c_{\text{act}} - k_-}{p\,1625}(c_G^{i-1} - c_G^i) \\
\dot{c}_S^i &= +k_{\text{cat}} c_G^i && -k_{\text{resc}} c_S^i && +\frac{k_{\text{depol}}}{p\,1625}(c_S^{i+1} - c_S^i) \qquad i = 1, 2, \ldots, 99 \\
\dot{c}_G^{100} &= -k_{\text{cat}} c_G^{100} && +k_{\text{resc}} c_S^{100} && +\frac{k_+ c_{\text{act}} - k_-}{p\,1625}(c_G^{99} - c_G^{100}) \\
\dot{c}_S^{100} &= +k_{\text{cat}} c_G^{100} && -k_{\text{resc}} c_S^{100} && +\frac{k_+ c_{\text{act}} - k_-}{p\,1625} c_G^{100} \qquad -\frac{k_{\text{depol}}}{p\,1625} c_S^{100} \\
\dot{c}_G &= -k_{\text{cat}} c_G && +k_{\text{resc}} c_S && -\frac{k_+ c_{\text{act}} - k_-}{p\,1625}(c_G^{100} - c_G^0) \\
\dot{c}_S &= +k_{\text{cat}} c_G && -k_{\text{resc}} c_S && -\frac{k_+ c_{\text{act}} - k_-}{p\,1625} c_G^{100} \qquad -\frac{k_{\text{depol}}}{p\,1625} c_S^1 \\
\dot{c}_{\text{grw}} &= -k_{\text{cat}} c_{\text{grw}} && +k_{\text{resc}} c_{\text{shr}} && +(k_+ c_{\text{act}} - k_-)(c_G - 100 c_G^{100} + c_G^0) \\
\dot{c}_{\text{shr}} &= +k_{\text{cat}} c_{\text{grw}} && -k_{\text{resc}} c_{\text{shr}} && +(k_+ c_{\text{act}} - k_-)\,100 c_G^{100} \qquad -k_{\text{depol}} c_S \\
\dot{c}_{\text{oli}} &= -k_{\text{oli}} c_{\text{oli}} && && +k_{\text{depol}} c_S \\
\dot{c}_{\text{ina}} &= +k_{\text{oli}} c_{\text{oli}} && -k_{\text{exc}} c_{\text{exc}} && \\
\dot{c}_{\text{act}} &= && +k_{\text{exc}} c_{\text{exc}} && -(k_+ c_{\text{act}} - k_-)(c_G + c_G^0) \\
\dot{c}_{\text{GTP}} &= -k_{\text{spon}} c_{\text{GTP}} && -k_{\text{exc}} c_{\text{exc}} && 
\end{aligned}
$$

Extension of the MTOSC system on differential equations by explicit length distributions of *G*- and *S*-MTs. The length distributions are approximated by 100 discrete values for *G*-MTs and another 100 values for *S*-MTs. $c_G^i$ and $c_S^i$ ($i = 1, 2, \ldots, 100$) are the number concentration of *G*- and *S*-MTs, respectively, of lengths between $(i-1) \cdot$ p and $i \cdot p$ μm ($p$: positive real number). $c_G^0$ is the number concentration of nuclei. The other variables have the same meaning as in Table 1. The upper block contains the time derivatives of the new variables. Nuclei are not counted with MTs, i.e. $c_G = c_G^1 + c_G^2 + \ldots + c_G^{100}$, but elongation of nuclei is described by separate expressions. The number concentrations $c_G^i$ change by catastrophe and rescue, as well as by MT elongation. To avoid cut-off errors, growing MTs of the maximal length are assumed to undergo catastrophe instead of further elongation. Similarly, the equations for the $c_S^i$ contain terms for catastrophe, rescue, and rapid shortening. The second block corresponds to the MTOSC system of differential equations. MT100 contains an additional equation for the dimer equivalent concentration of growing MTs, $c_{\text{grw}}$. By introduction of the length distribution variables, the variables $c_G$, $c_S$, $c_{\text{grw}}$, and $c_{\text{shr}}$ become redundant; they are enclosed in the MT100 system for computing time minimization and are used to control the accuracy of the numeric solutions

troduced for the number concentration of nuclei. Throughout the equations, nuclei are treated separately from MTs. (Otherwise, we had to distinguish between growing and shortening nuclei.) Thus, the total number concentration of *G*-MTs is

$$c_G = c_G^1 + c_G^2 + \ldots + c_G^{100} .$$

In all other aspects, nuclei are considered as *G*-MTs of zero length.

The number concentration $c_G^i$ ($i = 1, 2, \ldots, 99$) changes by catastrophe, rescue, and elongation. The latter effect gives a positive contribution which is proportional to $c_G^{i-1}$, the number concentration of *G*-MTs just growing into the length segment $i$, and a negative contribution proportional to $c_G^i$ itself, because these MTs are growing out of the $i$-th length segment. The proportionality factor, i.e., the rate constant for changes of the number concentrations due to elongation, is the net dimer association rate constant, $k_+ \cdot c_{\text{act}} - k_-$, divided by the number of dimers in a MT-segment of lengths $p$ μm. The case $k_+ \cdot c_{act} - k_- < 0$ is considered to be irrelevant, since *G*-MTs then loose their caps and change to the *S*-state (short caps assumed). Thus, in realistic simulations, *G*-MTs will always be growing.

The equations for the number concentrations of *S*-MTs are deduced in the same way. For reasons of numerical consistency, *G*-MTs of the maximal length (100 $p$ μm) are supposed to convert to the *S*-state upon elongation. This artificial assumption does no harm as long as $p$ is sufficiently large.

Besides the equations for MT length distributions (represented by the variables $c_G^i$ and $c_S^i$), MT100 contains equations for the total number concentrations $c_G$ and $c_S$ of *G*- and *S*-MTs. Thus, the MT100 system of differential equations is redundant. One reason for including these equations is to save computing time. Otherwise, summations over all $c_G^i$ and $c_S^i$ would be necessary each time the equations in Table 3 have to be evaluated. Another advantage is that redundancy can be used to monitor the accuracy of numerical integrations by comparing the to-

tal number concentrations with the corresponding sums of the $c_G^i$'s and $c_S^i$'s. For the same reasons, equations for the concentrations of dimers in the form of *G*- and *S*-MTs, $c_{grw}$ and $c_{shr}$, have been included.

*The evolution of MT length distributions*

The accuracy of the approximation used for the quasi-continuous length distributions depends on the step size *p*. Therefore, *p* should be as small as possible. In most cases, approximation by 100 discrete values seems to be more than sufficient. However, within the framework of the MT100 model, the step size has also influence on the evolution of the length distributions in time. The terms

$$(k_+ c_{act} - k_-)(c^{i-1}\hat{G} - c^i \hat{G})/(p \cdot 1625)$$

and

$$k_{depol}(c^{i+1}\hat{S} - c^i \hat{S})/(p \cdot 1625),$$

describing the changes of the number concentrations by elongation or depolymerization, guarantee that *on average*, MTs grow or shorten at the expected rates. But the shape of the length distributions changes differently, depending on the value of the step size. Given a set of *G*-MTs, for instance, with all MTs being of the same length at an initial time $t_1$, then at a later time $t_2$, when the MTs have on average elongated by *m* steps ($=m \cdot p$ μm), the width of the length distribution is $\sqrt{m}$ steps (standard deviation) or $p\sqrt{m}$ μm. (Nucleation and catastrophe are neglected for the moment; for a more rigorous discussion of length distribution kinetics see Kristofferson et al. 1980). This is demonstrated in Fig. 7. Thus, the length distributions change as if elongation and shortening occurred by blockwise addition and dissociation of p · 1625 dimers.

It is a common assumption of most models that MTs grow by association of single dimers. Thus, the natural step size (for elongation at least) seems to be very small: $p = 1/1625$, corresponding to one single dimer. Starting with a set of MTs of equal lengths (nuclei, for instance), this would evolve into an extremely narrow length distribution after some time of elongation. According to Poisson statistics, the half-width would be $(m_+)^{1/2} + (m_-)^{1/2}$ dimers, where $m_+$ and $m_-$ are the numbers of association and dissociation events during the time of growth. Neglecting the dissociation events (this might be justified for fast growth, at high TU · GTP concentrations), this means that after growth of 1 μm (10 μm), the half-width is 0.025 μm (0.078 μm). Consequently, at the scale of light microscopy, the growth rate would be quite constant (at constant $c_{act}$).

However, MTs grow and shorten at variable rates (c.f. Gildersleeve et al. 1992). It is not yet clear whether or not the different rates must be ascribed to different dynamic states. At least formally, the variability could be taken into account by using suitable step sizes for elongation and shortening. In order to test whether consideration of explicit length distributions change the predictions of our model, we used equal steps for growth and shortening, starting with quite large steps of the order of 1 μm (i.e. packages of 1625 dimers; corresponding to 100 steps at a maximal MT length of 100 μm). Deviations between the results obtained by MTOSC and MT100 are quite marginal (c.f. Fig. 4).

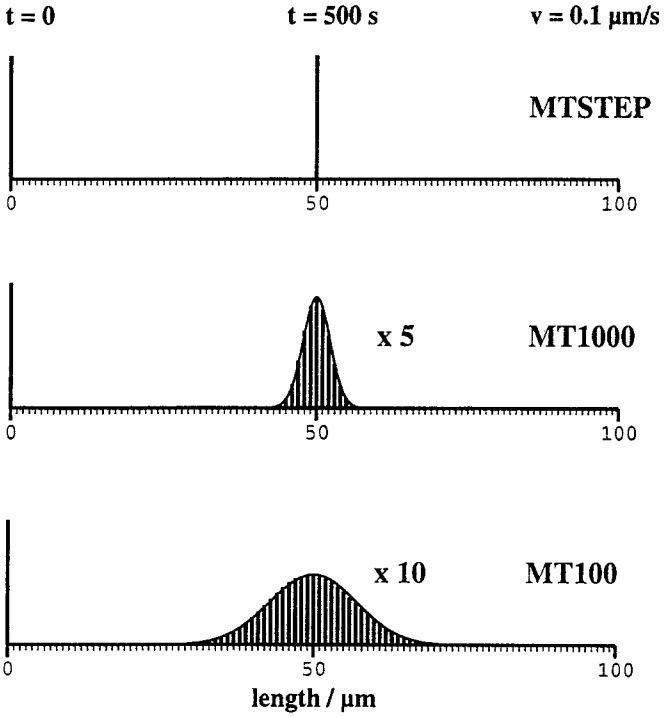


**Fig. 7.** MT-length distributions (histograms, 1 μm intervals) according to MT100, MT1000, and MTSTEP, calculated for MTs after 500 s of growth at constant velocity, $v = 0.1$ μm/s; MTs are assumed to start at $t = 0$ with zero length (nuclei, represented by single bars at the left end). Rates of nucleation and catastrophe are set to zero. Constant growth is assured by changing the time derivative of $c_{act}$ to $dc_{act}/dt = 0$. $v = (k_+ \cdot c_{act} - k_-)/(1625$ dimers/μm), with $k_+ = 10\ \mu M^{-1}\ s^{-1}$, $k_- = 45\ s^{-1}$, and $c_{act} = 20.75$ μM. The continuous lines show the distributions that are expected for MT elongation by stochastic addition of packages of 1625 dimers (blocks of 1 μm length as assumed by MT100) and of 162.5 dimers (blocks of 0.1 μm lenghts as assumed by MT1000). The discrete Poisson distributions are approximated by Gaussians. Bars and lines have been rescaled by the factors indicated. For stochastic association and dissociation of single dimers, the expected length distribution is very narrow (standard deviation is 472 dimers, corresponding to 0.29 μm). It is best represented by MTSTEP

*Extrapolation to small step sizes: MT1000*

In order to slow down broadening of the length distributions, we decreased the step size by a factor of 10 by increasing the number of the variables $c_G^i$ and $c_S^i$ from 100 to 1000, leading to a system of 2009 equations (MT1000) instead of 209 equations (MT100). (With less spreading of the length distributions, the upper limit of MT lengths can be lowered, allowing additional reduction of the step size *p*.) The results do not differ significantly from those of the MT100 calculations. Although the number of dimers per package is still of the order of 100, it seems not justified to expect fundamental changes of polymerization kinetics in the limit of one dimer per step.

*Hybrid model without spreading: MTSTEP*

To safely exclude the possibility of length distribution effects at small step sizes, spreading because of MT elongation should be minimized by using single dimer steps. But a further increase of the number of variables describing the length distributions is no practical way. Thus, in another formulation of the reaction model, MTSTEP, we used an approach which totaly avoids spreading of length distributions caused by fluctuations in growth and shortening. MTSTEP uses a set of equations similar to that of MT1000, but without the terms describing the changes of the $c_G^i$ and $c_S^i$ due to elongation and shortening. The set of differential equations is solved numerically for small time intervals corresponding to a shortening distance (for *S*-MTs) of $p$ μm (one step) or integer fractions of that; at the ends of these time intervals, the length distribution of *S*-MTs is updated by an appropriate shift of the contents of the variables $c_S^i$. An additional variable is introduced which records the length of a hypothetical MT that keeps on growing, irrespective of catastrophe and rescue. (A similar variable to monitor the distance of shortening is not necessary because the rate of shortening is constant in time.) If the recorded growth distance has increased by at least $p$ μm since last $c_G^i$-update, the length distribution of growing MTs is also updated. As expected, the difference between the solutions of MTSTEP and MT1000 is negligible (s. Fig. 4).

## References


Bayley PM, Manser EJ (1985) Assembly of microtubules from nucleotide-depleted tubulin. Nature 318:683–685

Bayley PM, Martin SR (1986) Inhibition of microtubule elongation by GDP. Biochem Biophys Res Commun 137:351–358

Bayley PM, Schilstra MJ, Martin SR (1989) A simple formulation of microtubule dynamics: quantitative implications of the dynamic instability of microtubule populations in vivo and in vitro. J Cell Sci 93:241–254

Bayley P, Schilstra M, Martin S (1989a) A lateral cap model of microtubule dynamic instability. FEBS Lett 259:181–184

Bayley PM, Schilstra MJ, Martin SR (1990) Microtubule dynamic instability: numerical simulation of microtubule transition properties using a lateral cap model. J Cell Sci 95:33–48

Boulin C, Kempf R, Koch M, McLaughlin S (1986) Data appraisal, evaluation and display for synchrotron radiation experiments: hardware and software. Nucl Instrum Methods A 249:399–407

Caplow M (1992) Microtubule dynamics. Curr Opinion Cell Biol 4:58–65

Carlier M-F, Pantaloni D (1981) Kinetic analysis of guanosine 5′-triphosphate hydrolysis associated with tubulin polymerization. Biochemistry 20:1918–1924

Carlier M-F, Melki R, Pantaloni D, Hill TL, Chen Y (1987) Synchronous oscillations in microtubule polymerization. Proc Natl Acad Sci, USA 84:5257–5261

Carlier MF, Didry D, Melki R, Chabre M, Pantaloni D (1988) Stabilization of microtubules by inorganic phosphate and its structural analogues, the fluoride complexes of aluminum and beryllium. Biochemistry 27:3555–3559

Cassimeris L, Pryer NK, Salmon ED (1988) Real-time observation of microtubule dynamic instability in living cells. J Cell Biol 107:2223–2231

Chen Y, Hill TK (1985) Monte Carlo study of the GTP cap in a five-start helix model of a microtubule. Proc Natl Acad Sci, USA 82:1131–1135

Chen Y, Hill TL (1987) Theoretical studies on oscillations in microtubule polymerization. Proc Natl Acad Sci, USA 84:8419–8423

Chretien D, Metoz F, Verde F, Karsenti E, Wade RH (1992) Lattice defects in microtubules: protofilament numbers vary within individual microtubules. J Cell Biol 117:1031–1040

Coue M, Lombillo VA, McIntosh JR (1991) Microtubule depolymerization promotes particle and chromosome movement in vitro. J Cell Biol 112:1165–1175

Drechsel DN, Hyman AA, Cobb MH, Kirschner MW (1992) Modulation of the dynamic instability of tubulin assembly by the microtubule-associated protein tau. Mol Biol Cell 3:1141–1154

Engelborghs Y, Eccleston J (1982) Fluorescence stopped-flow study of the binding of S6-GTP to tubulin. FEBS Lett 141:78–81

Erickson HP, O'Brien ET (1992) Microtubule dynamic instability and GTP hydrolysis. Annu Rev Biophys Biomol Struct 21:145–166

Gaskin F, Cantor CR, Shelanski MI (1974) Turbidimetric studies of the in vitro assembly and disassembly of porcine neurotubules. J Mol Biol 89:737–758

Gildersleeve RF, Cross AR, Cullen KE, Fagen AP, Williams RC (1992) Microtubules grow and shorten at intrinsically variable rates. J Biol Chem 267:7995–8006

Hamel E, Batra J, Lin C (1986) Direct incorporation of guanosine 5′-diphosphate into microtubules without guanosine 5′-triphosphate hydrolysis. Biochemistry 25:7054–7062

Hill TL, Chen Y (1984) Phase changes at the end of a microtubule with a GTP cap. Proc Natl Acad Sci, USA 81:5772–5776

Hitt AL, Cross AR, Williams RC (1990) Microtubule solutions display nematic liquid-crystalline structure. J Biol Chem 265:1639–1647

Horio T, Hotani H (1986) Visualization of the dynamic instability of individual microtubules by dark-field microscopy. Nature 321:605–607

Howard WD, Timasheff SN (1986) GDP state of tubulin: stabilization of double rings. Biochemistry 25:8292–8300

Hyman AA, Salser S, Drechsel DN, Unwin N, Mitchison TJ (1992) Role of GTP hydrolysis in microtubule dynamics: information from a slowly hydrolysable analogue, GMPCPP. Mol Biol Cell 3:1155–1167

Koch MHJ, Bordas J (1983) X-ray diffraction and scattering on disordered systems using synchrotron radiation. Nucl Instrum Methods 208:461–469

Koshland DE, Mitchison TJ, Kirschner MW (1988) Polewards chromosome movement driven by microtubule depolymerization in vitro. Nature 331:499–504

Kristofferson D, Karr TL, Purich DL (1980) Dynamics of linear protein polymer disassembly. J Biol Chem 255:8567–8572

Lange G, Mandelkow E-M, Jagla A, Mandelkow E (1988) Tubulin oligomers and microtubule oscillations – antagonistic role of microtubule stabilizers and destabilizers. Eur J Biochem 178:61–69

Lin CM, Hamel E (1987) Interrelationships of tubulin-GDP and tubulin-GTP in microtubule assembly. Biochemistry 26:7173–7182

Mandelkow E, Mandelkow EM, Bordas J (1983) Synchrotron radiation as a tool for studying microtubule self-assembly. TIBS 8:374–377

Mandelkow E-M, Mandelkow E (1992) Microtubule oscillations. Cell Motility Cytoskeleton 22:235–244

Mandelkow E-M, Harmsen A, Mandelkow E, Bordas J (1980) X-ray kinetic studies of microtubule assembly using synchrotron radiation. Nature 287:595–599

Mandelkow E-M, Herrmann M, Rühl U (1985) Tubulin domains probed by subunit-specific antibodies and limited proteolysis. J Mol Biol 185:311–327

Mandelkow E-M, Lange G, Jagla A, Spann U, Mandelkow E (1988) Dynamics of the microtubule oscillator: role of nucleotides and tubulin-MAP interactions. EMBO J 7:357–365

Mandelkow E-M, Mandelkow E, Milligan RA (1991) Microtubule dynamics and microtubule caps: a time-resolved cryo-electron microscopy study. J Cell Biol 114:977–991

Martin SR, Bayley PM (1987) Effects of GDP on microtubules at steady state. Biophys Chem 27:67–76
Martin SR, Schilstra MJ, Bayley PM (1991) Opposite-end behaviour of dynamic microtubules. Biochim Biophys Acta 1073:555–561
Martin SR, Schilstra MJ, Bayley PM (1993) Dynamic instability of microtubules: Monte Carlo simulation and application to different types of microtubule lattice. Biophys J 65:578–596
Marx A, Jagla A, Mandelkow E (1990) Microtubule assembly and oscillations induced by flash photolysis of caged-GTP. Eur Biophys J 19:1–9
Melki R, Carlier M-F, Pantaloni D (1988) Oscillations in microtubule polymerization: the rate of GTP regeneration on tubulin controls the period. EMBO J 7:2653–2659
Melki R, Carlier M-F, Pantaloni D, Timasheff SN (1989) Cold depolymerization of microtubules to double rings: geometric stabilization of assemblies. Biochemistry 28:9143–9152
Mitchison T, Kirschner M (1984) Dynamic instability of microtubule growth. Nature 312:237–242
Obermann H, Mandelkow E-M, Lange G, Mandelkow E (1990) Microtubule oscillations: role of nucleation and microtubule number concentration. J Biol Chem 265:4382–4388
Obermann-Pleß H (1992) Zusammenhänge zwischen Nukleation, dynamischer Instabilität und Oszillationen von Mikrotubuli. Doctoral thesis, Hamburg
O'Brien ET, Voter WA, and Erickson HP (1987) GTP hydrolysis during microtubule assembly. Biochemistry 26:4148–4156
O'Brien ET, Salmon ED, Walker RA, Erickson HP (1990) Effects of magnesium on the dynamic instability of individual microtubules. Biochemistry 29:6648–6656
Pirollet F, Job D, Margolis RL, Garel J-R (1987) An oscillatory mode for microtubule assembly. EMBO J 6:3247–3252
Press WH, Flannery BP, Teukolsky SA, Vetterling WT (1988) Numerical recipes. Cambridge University Press, Cambridge
Pryer NK, Walker RA, Skeen VP, Bourns BD, Soboeiro MF, Salmon ED (1992) Brain microtubule-associated proteins modulate microtubule dynamic instability in vitro. J Cell Sci 103:965–976
Renner W, Mandelkow E-M, Mandelkow E, Bordas J (1983) Self-assembly of microtubule protein studied by time-resolved X-ray scattering using temperature jump and stopped flow. Nucl Instrum Methods 208:535–540
Rothwell SW, Grasser WA, Baker HN, Murphy DB (1987) The relative contributions of polymer annealing and subunit exchange to microtubule dynamics in vitro. J Cell Biol 105:863–874
Sammak PJ, Borisy GG (1988) Direct observation of microtubule dynamics in living cells. Nature 332:724–726
Schilstra MJ, Martin SR, Bayley PM (1987) On the relationship between nucleotide hydrolysis and microtubule assembly: Studies with a GTP-regenerating system. Biochem Biophys Res Commun 147:588–595
Schulze E, Kirschner M (1988) New features of microtubule behavior observed in vivo. Nature 334:356–359
Smith P, Krohn I, Hermanson G, Malla A, Gartner F, Provenzano M, Fujimoto E, Goeke N, Olson B, Klenk D (1985) Measurement of protein using bicinchoninic acid. Anal Biochem 150:76–85
Somers M, Engelborghs Y (1990) Kinetics of the spontaneous organization of microtubules in solution. Eur Biophys J 18:239–244
Spann U, Renner W, Mandelkow E-M, Bordas J, Mandelkow E (1987) Tubulin oligomers and microtubule assembly studied by time-resolved X-ray scattering: separation of prenucleation and nucleation events. Biochemistry 26:1123–1132
Stewart RJ, Farell KW, Wilson L (1990) Role of GTP hydrolysis in microtubule polymerization: evidence for a coupled hydrolysis mechanism. Biochemistry 29:6489–6498
Tabony J, Job D (1990) Spatial structures in microtubular solutions requiring a sustained energy source. Nature 346:448–451
Tabony J, Job D (1992) Gravitational symmetry-breaking in microtubular dissipative structures. Proc Natl Acad Sci, USA 89:6948–6952
Trinczek B, Marx A, Mandelkow E-M, Murphy DB, Mandelkow E (1993) Dynamics of microtubules from erythrocyte marginal bands. Mol Biol Cell 4:323–335
Voter WA, Erickson HP (1984) The kinetics of microtubule assembly: evidence for a two-stage nucleation mechanism. J Biol Chem 259:10430–10438
Voter WA, O'Brien ET, Erickson HP (1991) Dilution-induced disassembly of microtubules: relation to dynamic instability and the GTP cap. Cell Motility & Cytoskeleton 18:55–62
Wade RH, Pirollet F, Margolis RL, Garel J-R, Job D (1989) Monotonic versus oscillating microtubule assembly: a cryo-electron microscope study. Biol Cell 65:37–44
Walker RA, O'Brien ET, Pryer NK, Soboeiro M, Voter WA, Erickson HP, Salmon ED (1988) Dynamic instability of individual microtubules analysed by video light microscopy: rate constants and transition frequencies. J Cell Biol 107:1437–1448
Walker RA, Pryer NK, Salmon ED (1991) Dilution of individual microtubules observed in real-time in vitro: evidence that cap size is small and independent of elongation rate. J Cell Biol 114:73–81
Zeeberg B, Cheek J, Caplow M (1980) Exchange of tubulin dimer into rings in microtubule assembly-disassembly. Biochemistry 19:5078–5086